International Journal of Mechanical, Industrial and Aerospace Sciences
ISSN: 2517-9950
Vol:10, No:3, 2016

Wetting Characterization of High Aspect Ratio Nanostructures by Gigahertz Acoustic Reflectometry

C. Virgilio, J. Carlier, P. Campistron, M. Toubal, P. Garnier, L. Broussous, V. Thomy, B. Nongaillard

***Abstract*—**Wetting efficiency of microstructures or nanostructures patterned on Si wafers is a real challenge in integrated circuits manufacturing. In fact, bad or non-uniform wetting during wet processes limits chemical reactions and can lead to non-complete etching or cleaning inside the patterns and device defectivity. This issue is more and more important with the transistors size shrinkage and concerns mainly high aspect ratio structures. Deep Trench Isolation (DTI) structures enabling pixels' isolation in imaging devices are subject to this phenomenon. While low-frequency acoustic reflectometry principle is a well-known method for Non Destructive Test applications, we have recently shown that it is also well suited for nanostructures wetting characterization in a higher frequency range. In this paper, we present a high-frequency acoustic reflectometry characterization of DTI wetting through a confrontation of both experimental and modeling results. The acoustic method proposed is based on the evaluation of the reflection of a longitudinal acoustic wave generated by a 100 µm diameter ZnO piezoelectric transducer sputtered on the silicon wafer backside using MEMS technologies. The transducers have been fabricated to work at 5 GHz corresponding to a wavelength of 1.7 µm in silicon. The DTI studied structures, manufactured on the wafer frontside, are crossing trenches of 200 nm wide and 4 µm deep (aspect ratio of 20) etched into a Si wafer frontside. In that case, the acoustic signal reflection occurs at the bottom and at the top of the DTI enabling its characterization by monitoring the electrical reflection coefficient of the transducer. A Finite Difference Time Domain (FDTD) model has been developed to predict the behavior of the emitted wave. The model shows that the separation of the reflected echoes (top and bottom of the DTI) from different acoustic modes is possible at 5 Ghz. A good correspondence between experimental and theoretical signals is observed. The model enables the identification of the different acoustic modes. The evaluation of DTI wetting is then performed by focusing on the first reflected echo obtained through the reflection at Si bottom interface, where wetting efficiency is crucial. The reflection coefficient is measured with different water / ethanol mixtures (tunable surface tension) deposited on the wafer frontside. Two cases are studied: with and without PFTS hydrophobic treatment. In the untreated surface case, acoustic reflection coefficient values with water show that liquid imbibition is partial. In the treated surface case, the acoustic reflection is total with water (no liquid in DTI). The impalement of the liquid occurs for a specific surface tension but it is still partial for pure ethanol. DTI bottom shape and local pattern collapse of the trenches can explain these incomplete wetting phenomena. This high-frequency acoustic method sensitivity coupled with a FDTD propagative model thus enables the local determination of the wetting state of a liquid on real structures. Partial wetting states for non-hydrophobic surfaces or low surface tension liquids are then detectable with this method.

***Keywords*—**Wetting, acoustic reflectometry, gigahertz, semiconductor.

C. Virgilio, J. Carlier, P. Campistron, M. Toubal and B. Nongaillard are with the Université de Valenciennes et du Hainaut-Cambrésis, Institute of Electronics, Microelectronics and Nanotechnology, IEMN, UMR 8520, Le Mont Houy 59313, France (e-mail: christophe.virgilio@gmail.com).

P. Garnier and L. Broussous are with STMicroelectronics, Crolles, 38926, France.

V. Thomy is with the Institute of Electronics, Microelectronics and Nanotechnology, Univ. Lille, UMR 8520 - IEMN, F-59000 Lille, France.

I. Introduction

DEEP trench structures with high aspect ratios appear in different semiconductor technologies like DRAM, NAND 3D memories and imaging devices. With node evolution and the miniaturization of the components, their aspect ratios are becoming higher and higher. In the 1990s, deep trenches of 4 µm and 0.5 µm wide were used in DRAM memories. Nowadays, they are 18 nm wide with aspect ratios up to 100. Efficient wet etching or cleaning of these structures is determined by a complete wetting of the patterns which is very challenging at the nanometer scale [1] and an adequate drying to avoid pattern collapse. Advanced drying methods exist to solve the latter problem like the use of supercritical CO_2 or freeze /sublimation of the cleaning solvent [2], [3]. However, fewer works concerning pattern wetting and cleaning efficiency of real structures have been undertaken. In fact, wetting characterization of real structures at the nanometer scale is limited due to the lack of efficient methods. Goniometric optical methods make it possible to evaluate the wetting of a droplet on nanostructures, but this characterization is limited to the droplet rim, where the triple line is defined. On the micro/nanometer scale, the liquid/solid/gas interface can be characterized by different methods with huge accuracy [4]–[9]. Cassie state (liquid droplet stands on top of the roughness trapping air pockets between the asperities) and Wenzel state (liquid imbibition is complete) are detectable with these methods but few of them are compatible with an in situ, real time and multiscale (from macro to nanoscale) characterization. High-frequency acoustic reflectometry has been recently used to characterize the wetting of silicon hydrophobic micro-pillars [10] and nano-pillars [11]. These studies showed that this method is particularly sensitive to the different states of wetting of a droplet on a patterned surface. Moreover, intermediate wetting states (non-filling of all asperities by the liquid) can also be identified because the determination of the wetting state is directly performed under the droplet, at the vertical of the transducer. The method accuracy is comparable to the one of recent studies of nanostructures wetting using optical reflectance measurements [12] or attenuated total reflection infra-red spectroscopy [13]. Another acoustic method using the response of a quartz crystal microbalance [14], [15] also

enables Cassie or Wenzel state detection but patterns need to be manufactured directly on top of the sensor.

In our study, we will focus on the wetting characterization of Deep Trench Isolation structures (DTI) by Gigahertz acoustic reflectometry. A good cleaning of these structures is particularly important to avoid display issues like the apparition of white pixels on images (Fig. 1). The characterization will be performed with and without PFTS (1H,1H,2H,2H-perfluorodecyltrichlorosilane) hydrophobic treatment to have two different silicon surface energies (Young angle for water from 70° to 105°) for different ethanol / water mixtures to tune the surface tension of the wetting solution (with no major changes in viscosity). A Finite Difference Time Domain (FDTD) model has been developed offering a better understanding of the acoustic measurements. It enables the determination of the optimum frequency range according to the geometry of the structure under investigation.

Fig. 1 Metallic ions contamination in DTI leading to the apparition of white pixels

II. Experimental

A. DTI Geometry

All the DTI structures are etched on the frontside of a 300 mm silicon wafer of 775 µm in thickness and fabricated by STMicroelectronics. They consist of a three dimensional network of crossing trenches of about 200 nm wide and 4 µm deep patterned on a Si / SiO_2 pad oxide (75 Å) / SiN hardmask (800 Å) stack (Fig. 2).

B. Acoustic Echography Method

The technique consists in the evaluation of the reflection of a high-frequency longitudinal acoustic wave (gigahertz range) on the structured interface (DTI) between bare silicon and a liquid droplet (Fig. 3).

An acoustic wave is generated by piezoelectric transducers fabricated on the wafers backside. A ground electrode is first deposited on silicon by thermal evaporation (Ti / Pt: 10 nm / 50 nm). The shape and size of the transducers are then designed by a photolithography step (a circle with diameter of 100 µm) and ZnO is deposited by magnetron sputtering.

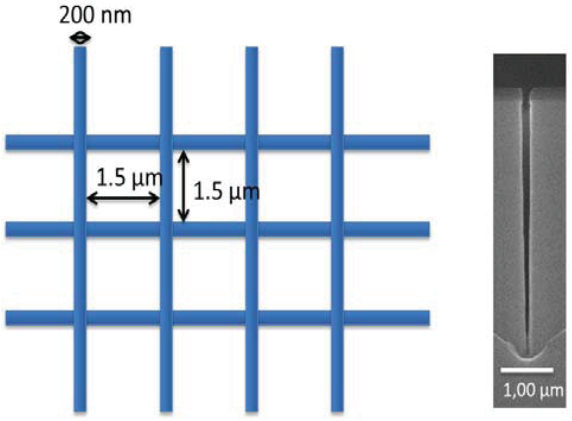

Fig. 2 (a) Scheme of the top view of the DTI structures (DTI in blue) (b) SEM cross section of one trench

The resonance frequency of the transducer is set by the thickness of the ZnO layer (650 nm for 3 GHz and 310 nm for 5 GHz). Finally, the top electrode is also deposited by thermal evaporation (Pt: 50 nm) and transducers are obtained thanks to lift off technique. All the materials thicknesses have been predicted by simulating the best combination of thicknesses to reach the maximum conversion of electrical energy into acoustic energy. The longitudinal wave reflection occurs at the interface between the silicon and the medium on the wafer frontside enabling its characterization by monitoring the transducer electrical impedance. In fact, the S11(f) scattering parameter (ratio of the complex amplitudes of the reflected and incident signals) is measured using a SussMicrotech probe coupled with a Rohde & Schwarz 300 kHz – 8 GHz vector network analyzer. The reflection coefficient is obtained by applying an inverse Fourier transform to the S11(f) to get the reflected echoes in the time domain S11(t). The amplitude of the signal is then normalized to air to get rid off the intrinsic insertion losses from the measurements.

All measurements are performed at 20°C with different ethanol / water mixtures (surface tension decreases with ethanol concentration increase) deposited on the wafer frontside. Two types of samples have been characterized: untreated DTI and DTI with a treatment generating hydrophobic surfaces. To modify the intrinsic wettability of the DTI, a self-assembled monolayer (SAM) of PFTS was grafted from the vapor phase to functionalize the silicon surface.

III. Results and Discussion

A. Measurements at 3 GHz

In a first place, the S11(t) parameter has been evaluated at 3 GHz on the frequency bandwidth [0.5 GHz; 5 GHz] without any liquid deposited on the surface (Fig. 4).

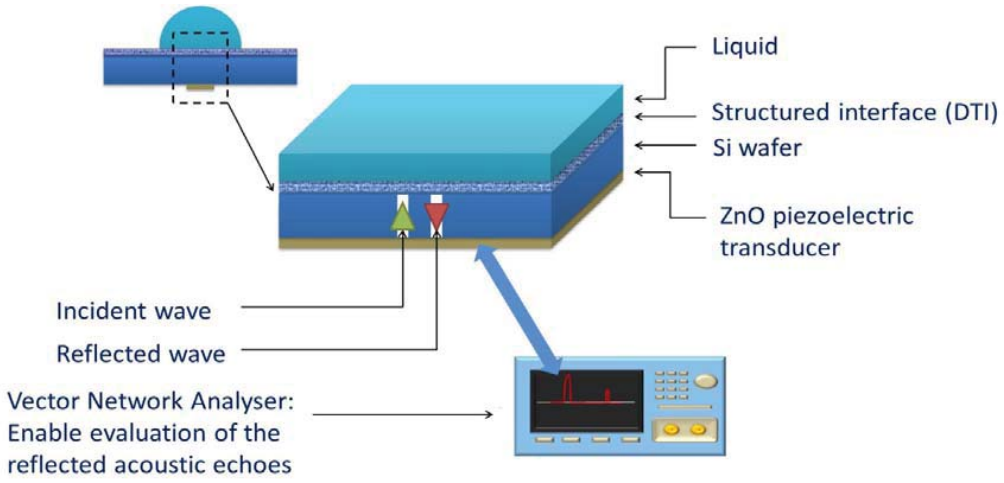

Fig. 3 High-frequency acoustic reflectometry principle

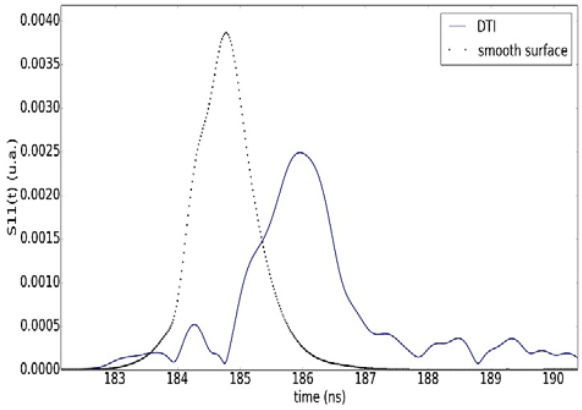

Fig. 4 Echoes diagram at air exposure at 3 GHz on the frequency bandwidth [0.5 GHz ; 5 GHz]

On the same sample, reflected acoustic echoes measurements are made for an etched area (DTI) and for a non-etched area (smooth surface). For the smooth surface, only one total acoustic reflection occurs at the interface between raw silicon and air. The exact thickness of the wafer "e" can be deduced from the echo position in time t_{smooth} as the longitudinal acoustic velocity in silicon c_l is known. It is calculated from (1) and we find a thickness of 778 µm (t_{smooth} = 184.7 ns and c_l = 8433 m.s^{-1})

$$e = 0.5 c_l t_{smooth} \quad (1)$$

For the DTI surface, some echoes appear at different time positions suggesting that a complex system of several waves with different velocities build up inside the DTI structure. No one perfectly matches with the one for the smooth surface, so no pure longitudinal wave propagation seems to exist at 3 GHz in the DTI network. The identification of the different modes is particularly difficult because a good separation in time of the different echoes is not possible. So, the wetting characterization cannot be performed (reflections on bottom and top of the DTI are not identified). This is due to the wavelength of the incident wave in the silicon (2.8 µm at 3 GHz) which is too close to the DTI thickness (4 µm). Consequently, a FDTD model has been developed to predict the resonant frequency needed to separate the echoes efficiently. It also enables to calculate the theoretical reflection coefficient on the bottom of the DTI in Cassie and Wenzel state with water.

B. FDTD Model

The real DTI network geometry has been simplified as it is very complex to encode (Fig. 5).

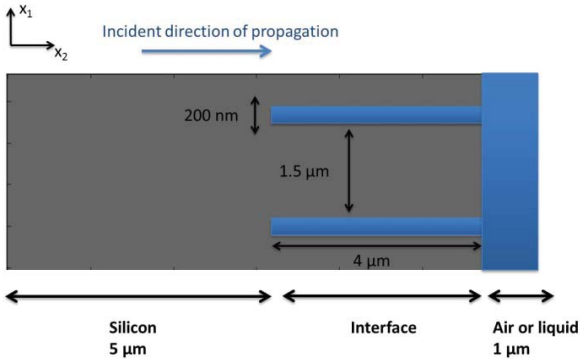

Fig. 5 Scheme of the geometry of the unit cell used for the FDTD model

The 3D-network of the real DTI structures is converted into a 2D-network composed of a quite simple unit cell which is periodized in the x1 direction with the real trench deepness (4 µm) and width (200 nm). The unit cell is then transformed into a rectangular mesh whose spatial period is directly based on the number of points per wavelength in the silicon. 640 points in the x_2 direction and 270 points in the x_1 direction have been taken for a frequency f_0 = 5 GHz (wavelength of 1.7 µm). The raw silicon thickness (5 µm) and the liquid thickness (1 µm) are chosen small to minimize the number of mesh points (reduction of calculating time). The excitation source is

obtained by the apodization of a sinus function. In the following equations, u_i and v_i are respectively the acoustic displacement and velocity in the i direction, (T_{11}, T_{12}, T_{22}), (c_{11}, c_{12}, c_{66}), (η_{11}, η_{12}, η_{66}), ρ the stress tensor components, the elastic constants, the viscosity constants and the density of the considered material, t the time, Δt the time step, Δx the spatial step, and (n, j) integers. For each variable X:

$$\frac{\partial X}{\partial x} = \frac{X(x=j+1) - X(x=j-1)}{2\Delta x} \tag{2}$$

In silicon at $x_2 = 0$ and for $t < 2/f_0$:

$$\left\{ \begin{array}{c} v_1^0 = 0 \\ v_2^0 = H(t)\sin(2\pi f t) \end{array} \right\} \tag{3}$$

Then, in each material, at $t = (2n + 1)\Delta t$, velocity field can be integrated so as to compute the stress field:

$$\left\{ \begin{array}{l} u_1^{2n+1} = u_1^{2n-1} + 2\Delta t.v_1^{2n} \\ u_2^{2n+1} = u_2^{2n-1} + 2\Delta t.v_2^{2n} \end{array} \right\}$$

$$\left\{ \begin{array}{l} v_1^{2n+1} = v_1^{2n} + \Delta t.incr_{v_1}^{2n} \\ v_2^{2n+1} = v_2^{2n} + \Delta t.incr_{v_2}^{2n} \end{array} \right\} \tag{4}$$

$$\left\{ \begin{array}{l} T_{11}^{2n+1} = C_{11}\frac{\partial u_1^{2n+1}}{\partial x_1} + C_{12}\frac{\partial u_2^{2n+1}}{\partial x_2} + \eta_{11}\frac{\partial v_1^{2n+1}}{\partial x_1} + \eta_{12}\frac{\partial v_2^{2n+1}}{\partial x_2} \\ T_{22}^{2n+1} = C_{12}\frac{\partial u_1^{2n+1}}{\partial x_1} + C_{11}\frac{\partial u_2^{2n+1}}{\partial x_2} + \eta_{12}\frac{\partial v_1^{2n+1}}{\partial x_1} + \eta_{11}\frac{\partial v_2^{2n+1}}{\partial x_2} \\ T_{12}^{2n+1} = C_{66}(\frac{\partial u_1^{2n+1}}{\partial x_2} + \frac{\partial u_2^{2n+1}}{\partial x_1}) + \eta_{66}(\frac{\partial v_1^{2n+1}}{\partial x_2} + \frac{\partial v_2^{2n+1}}{\partial x_1}) \end{array} \right\}$$

And, Newton law is applied to calculate the increments of the velocity field:

$$\left\{ \begin{array}{l} incr_{v_1}^{2n+1} = \frac{1}{\rho}(\frac{\partial T_{11}^{2n+1}}{\partial x_1} + \frac{\partial T_{12}^{2n+1}}{\partial x_2}) \\ incr_{v_2}^{2n+1} = \frac{1}{\rho}(\frac{\partial T_{12}^{2n+1}}{\partial x_1} + \frac{\partial T_{22}^{2n+1}}{\partial x_2}) \end{array} \right\} \tag{5}$$

Then, at $t = (2n + 2)\Delta t$, the velocity field is updated:

$$\left\{ \begin{array}{l} v_1^{2n+2} = v_1^{2n} + 2\Delta t.incr_{v_1}^{2n+1} \\ v_2^{2n+2} = v_2^{2n} + 2\Delta t.incr_{v_2}^{2n+1} \end{array} \right\} \tag{6}$$

The boundary conditions between the different materials are calculating according to Fig. 6. We use periodic boundary conditions at the top and the bottom and non-reflecting conditions for the right and left side of the meshed area [16], [17].

The acoustic velocity field is then available at any time and any spatial position. The simulated echoes diagram in the DTI case with air and a smooth surface is presented in Fig. 7.

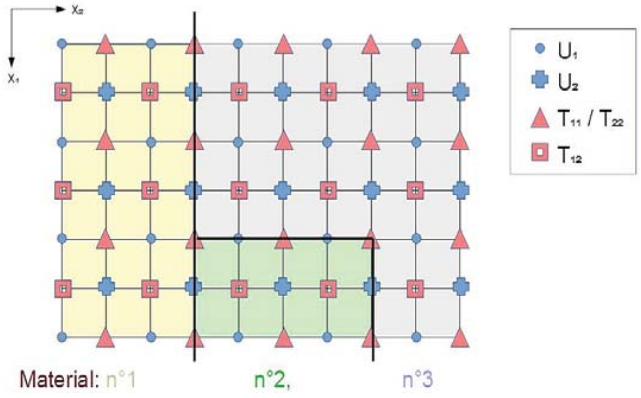

Fig. 6 Scheme of the boundary conditions calculation with 3 different materials in the mesh

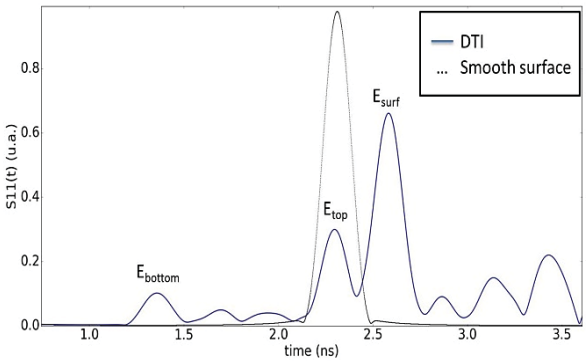

Fig. 7 Simulated echoes diagram at air exposure at 5 GHz

There are still different echoes for the DTI case but the separation between the echoes in the time domain is better than experimental 3 GHz case (Fig. 4). At 1.4 ns, a first echo is visible (E_{bottom}) which is well separated from the smooth case echo. This separation is very important for the wetting characterization because E_{bottom} will be characteristic of the reflection of the acoustic wave on the bottom of the DTI. We can also notice that the time position of the second echo at 2.3 ns (E_{top}) perfectly matches with the one of the smooth surface. A true longitudinal wave now exists inside the DTI structure. The last pretty good separated echo appearing at 2.6 ns (E_{surf}) is not useful for the wetting characterization but could be identified later thanks to the FDTD model. The reflection coefficients for the reflection E_{bottom} have been simulated for water in Cassie and Wenzel state. We find 1 (total reflection) for Cassie state and 0.858 for Wenzel state. These results have to be compared with experimental measurements of wetting at 5 GHz.

C. Measurements at 5 GHz

We decided to fabricate and use transducers working at 5 GHz which corresponds to a wavelength of 1.7 μm in the silicon on a higher frequency bandwidth [1 GHz; 8 GHz] to improve the separation of the reflected echoes in the time domain. Transducers with a higher resonant frequency than 5 GHz are unusable because their electrical impedance are too

small to have an accurate measurement of the S11(t) parameter with our experimental setup.

The S11(t) parameter has been evaluated at air exposure for DTI area and smooth area (Fig. 8). Even if the simulated network geometry is simplified, the global shape of the experimental and simulated echoes diagrams is very similar. At 183.3 ns, 184.3 ns and 185 ns E_{bottom}, E_{top} and E_{surf} are clearly identified.

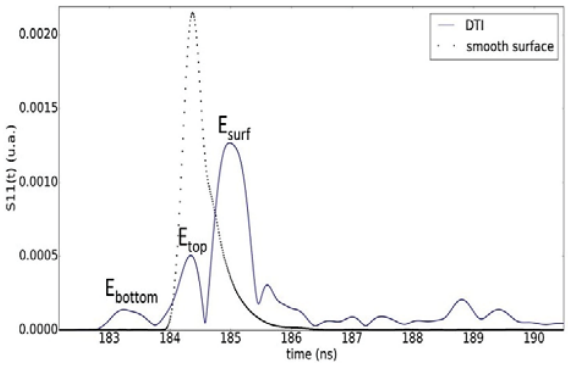

Fig. 8 Echoes diagram at air exposure at 5 GHz on the frequency bandwidth [1 GHz; 8 GHz]

Now that the reflection on the bottom of the DTI is experimentally identified, the acoustic reflection coefficient of R_{bottom} is measured for different ethanol / water mixtures with and without PFTS treatment of the DTI structures (Fig. 9).

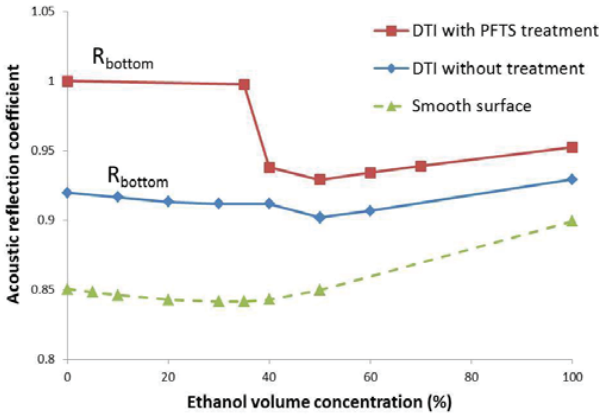

Fig. 9 Measured acoustic reflection coefficient for different ethanol / water mixtures

For the PFTS case, the reflection coefficient value is 1 with water which indicates that the liquid is in Cassie state. For an ethanol concentration between 30% and 50% which corresponds to a surface tension between 35.0 $mN.m^{-1}$ and 29.2 $mN.m^{-1}$, the reflection coefficient rapidly decreases from 1 to 0.93 which is characteristic of a Cassie / Wenzel transition [10]. Then, the slight increase observed for higher ethanol concentration is due to the variations of the acoustic impedance of the mixture. However, the values beyond the transition are higher than those measured for the smooth surface case and the simulated one with water. It means that air is still present in the network and wetting is partial. For the untreated case, the reflection coefficient is lower than the one corresponding to the treated case and there is no Cassie / Wenzel transition anymore. Its value is still higher than in the smooth surface case (in the whole ethanol concentration range). We can conclude that the total wetting of the network is never achieved in the two cases even with the lower surface tension liquid (21.7 $mN.m^{-1}$ for pure ethanol). This trend could be explained by the collapse of the thinnest part of the network (Fig. 10) and the V-shape of the bottom of the trenches (Fig. 2 (b)) making the liquid penetration harder in these areas.

Fig. 10 SEM top view of a DTI network with pattern collapse

IV. Conclusion

The wetting characterization of real DTI structures has been accomplished by the use of a gigahertz acoustic reflectometry method. Thanks to the development of a FDTD model, we have shown that increasing the resonance frequency of the piezoelectric transducers from 3 GHz to 5 GHz enables a very accurate wetting characterization at a micro/nanometer scale.

Acknowledgment

This work was supported by STMicroelectronics, the French Nord-Pas-de-Calais region, the RENATECH network and the NANO 2017 program.

References

[1] G. Vereecke et al, "Wetting Challenges in Cleaning of High Aspect Ratio Nano-Structures," *Solid State Phenom.* 2012, 195, 235−238.
[2] H.-W. Chen et al., *ECS Trans.*, 2013, 58(6): 205-211.
[3] H.-W. Chen et al., *ECS Trans.*, 2015, 69(8): 119-130.
[4] S. Moulinet, and D. Bartolo, "Life and death of a fakir droplet: Impalement transitions on superhydrophobic surfaces," *Phys. J. E*, 2007, 24, 251.
[5] H. Rathgen, and F. Mugele, "Microscopic shape and contact angle measurement at a superhydrophobic surface," *Faraday Discuss.*, 2010, 146, 49C.
[6] P. Papadopoulos, L. Mammen, X. Deng, D. Vollmer, and H. J. Butt, "How superhydrophobicity breaks down," *Proc. Natl. Acad. Sci. U.S.A.*, 2013, 110, 3254.
[7] K. Rykaczewski, T. Landin, M. Walker, J. H. Scott, and K. K. Varanasi, "Direct Imaging of Complex Nano-to Microscale Interfaces Involving Solid, Liquid, and Gas Phases," *ACS Nano*, 2012, 6, 9326.
[8] A. T. Paxson, and K. K. Varanasi, "Self-similarity of contact line depinning from textured surfaces," *Nat. Commun.*, 2013, 4, 1.
[9] J. C. Tuberquia, W. S. Song, and G. K. Jennings, "Investigating the Superhydrophobic Behavior for Underwater Surfaces Using Impedance-Based Methods," *Anal. Chem.*, 2011, 83 (16), pp 6184-6190

[10] N. Saad et al., "Characterization of the state of a droplet on a micro-textured silicon wafer using ultrasound," *Journal of Applied Physics*, 2012, 112, 104908.
[11] S. Li et al., "High-Frequency Acoustic for Nanostructure Wetting Characterization," *Langmuir*, 2014, 30, 7601−7608.
[12] X. Xu et al., "Capturing Wetting States in Nanopatterned Silicon," *ACS Nano*, 2014, 8 (1), pp 885-893.
[13] G. Vereeck et al., "Partial Wetting of Aqueous Solutions on High Aspect Ratio Nanopillars with Hydrophilic Surface Finish," *ECS Journal of Solid State Science and Technology*, 2014, 3 (1), pp 3095-3100.
[14] P. Roach, G. McHale, C. R. Evans, N. J. Shirtcliffe, and M. I. Newton, "Decoupling of the Liquid Response of a Superhydrophobic Quartz Crystal Microbalance," *Langmuir*, 2007, 23 (19), pp 9823-9830
[15] G. McHale, P. Roach, C. Evans, N. Shirtcliffe, S. Elliott, and M. Newton, from the 2008 IEEE International Frequency Control Symposium, from the, Honolulu, Hawaii, 19-21 May 2008, pp 698–704.
[16] J. Virieux, "P-SV wave propagation in heterogeneous media: Velocity-stress finite-difference method," *Geophysics*, 1986, Vol 51, n°4, pp 889-901.
[17] G. Mur, "Absorbing Boundary Conditions for the Finite-Difference Approximation of the Time-Domain EM Field Equations," *IEEE Trans. Electromagn. Compat.*, 1981, EMC-23, pp 377-382.